

**To Cite:** Onder, A. (2023). Preparation of Cationic Composite Hydrogel Improved by Activated Carbon and Its Use in Removal of Anionic Dye. *Journal of the Institute of Science and Technology, 13(3), 1902-1915.*

### Aktif Karbon ile Geliştirilmiş Katyonik Kompozit Hidrojelin Hazırlanması ve Anyonik Boya Uzaklaştırılmasında Kullanımı

Alper ONDER\*

#### Öne Çıkanlar:

- MO uzaklaştırılması için yeni bir adsorban olarak aktif karbon içeren katyonik kompozit hidrojel
- Maksimum MO adsorpsiyon kapasitesi 909,09 mg/g dir.
- Kompozit hidrojel, anyonik boyaların giderimi için önemli bir potansiyele sahiptir.

#### Anahtar Kelimeler:

- Kompozit hidrojel
- Aktif karbon
- Metil turuncu
- Adsorpsiyon izoterm
- Adsorpsiyon kinetik

#### ÖZET:

Kuarterner amonyum içeren suda çözünmeyen p(AETAC)/AC kompozit hidrojelleri [2-(Akriloloksi)etil]trimetilamonyum klorür (AETAC) ve aktif karbon (AC) ile serbest radikal polimerizasyonu yöntemiyle hazırlandı. Kompozit hidrojel Fourier Dönüşümlü Kızılötesi Spektroskopisi (FT-IR), Termogravimetrik analiz (TGA), X-Işını Kırınım (XRD) ve Taramalı elektron mikroskobu (SEM) yöntemleriyle karakterize edildi. Ek olarak, 50 mg, 75 mg, 100 mg ve 150 mg AC içeren p(AETAC)/AC kompozit hidrojellerinin deiyonize sudaki şişme davranışı incelendi. 75 mg AC içeren p(AETAC)/AC<sub>75</sub> kompozit hidrojelinin çeşitli sulardaki şişme kapasitesi belirlendi. p(AETAC)/AC<sub>75</sub> kompozit hidrojelinin MO adsorpsiyonunu etkileyen başlangıç boya konsantrasyonu, temas süresi, boya çözeltisinin pH'ı, adsorban miktarı ve sıcaklık parametreleri araştırıldı. Elde edilen adsorpsiyon verileri, Langmuir izoterm modeli ve PFO kinetik modeliyle uyum sağlar. p(AETAC)/AC<sub>75</sub> kompozit hidrojelinin Langmuir izotermine göre maksimum adsorpsiyon kabiliyetinin 909.09 mg/g olduğu belirlendi. p(AETAC)/AC<sub>75</sub> kompozit hidrojelinin MO boyar maddesinin adsorpsiyonu için  $\Delta H^\circ$  ve  $\Delta S^\circ$  değerleri sırasıyla  $22.25 \pm 1.43$  ve  $85.40 \pm 4.60$  olarak hesaplandı. Ek olarak, dört farklı sıcaklıkta sıfırdan küçük olan  $\Delta G^\circ$  değeri boya adsorpsiyonunun kendiliğinden olduğunu ifade eder. Elde edilen tüm verilere göre p(AETAC)/AC<sub>75</sub> kompozit hidrojelini anyonik boyar maddelerin sudan uzaklaştırılması için umut verici bir aday olarak kabul edilebilir.

### Preparation of Cationic Composite Hydrogel Improved by Activated Carbon and Its Use in Removal of Anionic Dye

#### Highlights:

- The cationic composite hydrogel with activated carbon as a novel adsorbent for MO removal
- The maximum MO adsorption capacity was 909.09 mg/g.
- The composite hydrogel has significant potential for the removal of anionic dyes.

#### Keywords:

- Composite hydrogel
- Active carbon
- Methyl orange
- Adsorption isotherm
- Adsorption kinetic

#### ABSTRACT:

Water-insoluble p(AETAC)/AC composite hydrogels containing quaternary ammonium were prepared by free-radical polymerisation method with [2-(Acryloyloxy)ethyl]trimethylammonium chloride (AETAC) and activated carbon (AC). The composite hydrogel was characterized by Fourier Transform Infrared Spectroscopy (FT-IR), Thermogravimetric analysis (TGA), X-Ray Diffraction (XRD), and Scanning Electron Microscopy (SEM) methods. In addition, the swelling behavior of p(AETAC)/AC composite hydrogels containing 50 mg, 75 mg, 100 mg, and 150 mg AC in deionized water was investigated. The swelling capacity of the p(AETAC)/AC<sub>75</sub> composite hydrogel containing 75 mg AC in various waters was determined. Initial dye concentration, contact time, pH of dye solution, amount of adsorbent, and temperature parameters affecting MO adsorption of p(AETAC)/AC<sub>75</sub> composite hydrogel were investigated. The obtained adsorption data agree with the Langmuir isotherm model and the PFO kinetic model. It was determined that the maximum adsorption ability of p(AETAC)/AC<sub>75</sub> composite hydrogel according to Langmuir isotherm was 909.09 mg/g.  $\Delta H^\circ$  and  $\Delta S^\circ$  values for the adsorption of MO dye-stuff of p(AETAC)/AC<sub>75</sub> composite hydrogel were calculated as  $22.25 \pm 1.43$  and  $85.40 \pm 4.60$ , respectively. In addition, the value of  $\Delta G^\circ$  less than zero at four different temperatures indicates that the dye adsorption is spontaneous. According to all the data obtained, p(AETAC)/AC<sub>75</sub> composite hydrogel can be considered a promising candidate for the removal of anionic dyestuffs from water.

Alper ONDER ([Orcid ID: 0000-0002-0775-0053](https://orcid.org/0000-0002-0775-0053)), Canakkale Onsekiz Mart University, Faculty of Science, Department of Chemistry, Inorganic Materials Laboratory, Canakkele, Türkiye

**Corresponding Author:** Alper ÖNDER, e-mail: alperonder@outlook.com

## INTRODUCTION

The most important threat to the existence of people around the world is the lack of sufficient potable water. According to the World Health Organization (WHO), 15% of people depend on surface water as a source of drinking water. WHO is working hard to solve the problem of potable water supply in the world (Anirudhan et al., 2022). In addition, for the accessibility of drinking water to the world, the United Nations (UN) has defined as the sixth sustainable development goal. Among the pollutants of drinking water, industrial dyes pose significant threats to the environment and human health (Anirudhan et al., 2022; Glaas-WHO, 2022). Dyes present in water can reduce the effect of sunlight on aquatic plants and thus affect the growth of living ecosystems. At the same time, industrial dyes can cause adverse effects on DNA in cells, various types of cancer, and toxicity (Xu et al., 2019; Chowdhury et al., 2020; Güngör & Ozay, 2022b).

Various physical, chemical and biological methods are used to remove industrial dyes from wastewater (Kim et al., 2023). Researchers are working on various techniques to purify contaminated water and make it portable for the world's population. Among these techniques, the adsorption method has come to the fore with its easy use, high feasibility, affordable cost, and sustainability aspects (Ozsoy et al., 2022; Kim et al., 2023). So far, various adsorbents have been used to remove organic dyes such as hydrogels, nanospheres, nanotubes, metal-organic framework (MOF), and composite hydrogels (Onder & Ozay, 2021; Güngör & Ozay, 2022a; Abutaleb et al., 2023; Ilgin et al., 2023). Composite hydrogels are materials prepared with a filler with a different chemical structure into a three-dimensional cross-linked polymer network with various functional groups (Sugawara et al., 2020). Composite hydrogels, which have high adsorption capacity and excellent swelling properties, have attracted the attention of researchers because of their functional ability and efficiency (Onder et al., 2023). Composite hydrogels can remove dyes in aqueous solutions through hydrophobic interactions, electrostatic interactions, hydrogen bonding, and ion exchange interactions between the dye molecules and the composite hydrogel (Jiang et al., 2018; Ozsoy et al., 2022; Onder et al., 2023). Quaternary ammonium ( $R_4N^+$ ) based composite hydrogels are cationic superabsorbents. Cationic composite polymers can be used to remove anionic dyes. [2-(Acryloyloxy)ethyl]trimethylammonium chloride (AETAC), which has a  $R_4N^+$  group in its structure, is an excellent monomer for the preparation of selective adsorbent materials for the removal of anionic dyes. Ozsoy et al. reported that the composite polymeric material they prepared with AETAC monomer has a significant potential for anionic dyestuff ARS (Ozsoy et al., 2022). Composite hydrogels prepared with various materials such as montmorillonite, clay, and active carbon have been studied in various application areas such as biomedical, environmental, and energy (Tian et al., 2010; Zhang et al., 2018; Rong et al., 2021; Singh et al., 2022). Active carbon (AC) is an important adsorption material thanks to its porous structure and various properties such as biocompatibility.

In this study, water-insoluble p(AETAC)/AC composite hydrogels containing  $R_4N^+$  group with four different amounts of active carbon were synthesized. The characterization of the prepared p(AETAC)/AC composite hydrogels was performed by FT-IR (Fourier Transform Infrared Spectroscopy), XRD (X-Ray Diffraction), TGA (Thermogravimetric analysis), and SEM (Scanning Electron Microscopy). The effects of AC amount on the swelling behavior of p(AETAC)/AC composite hydrogels were investigated. In addition, the swelling behavior of p(AETAC)/AC<sub>75</sub> composite hydrogels in various waters was investigated. The effects of initial dye concentration, pH, temperature, and adsorbent amount on azo dye anionic dye MO adsorption of p(AETAC)/AC<sub>75</sub>

composite hydrogel developed as anionic dye removal material were investigated. With the help of the obtained data, isotherm, kinetic and thermodynamic parameters were obtained.

## MATERIALS AND METHODS

In order to create the composite hydrogel, Sigma-Aldrich provided the AETAC monomer, N,N'-methylenebisacrylamide (MBA), ammonium persulfate (APS) initiator, and N,N,N',N'-tetramethylethylenediamine (TEMED) accelerator. AC with a surface area of 99.25 m<sup>2</sup>/g and an average pore radius of 1.73 nm was obtained from Kimetsan Co. Ltd (Ilgin et al., 2023). The anionic dye MO used in adsorption studies was obtained from Sigma-Aldrich. The concentrated hydrochloric acid (HCl, 36.5%) and sodium hydroxide (NaOH) used to prepare solutions with different pH were obtained from Sigma-Aldrich and Merck. Deionized water was used in all studies. Throughout the course of the investigation, every experiment was run three times.

In the AC and p(AETAC)/AC<sub>75</sub> composite hydrogel structural FT-IR spectra, a Perkin Elmer Spectrum 100 FT-IR device was employed. The Swollen p(AETAC)/AC<sub>75</sub> composite hydrogel was lyophilized and surface morphology was performed with the FEI Quanta FEG 250 model SEM device. Thermal analysis of AC and p(AETAC)/AC<sub>75</sub> composite hydrogel was completed with Perkin Elmer brand TGA 8000 model instrument (30–1000 °C, 10 °C/min, nitrogen gas). XRD analyses of AC and p(AETAC)/AC<sub>75</sub> composite hydrogel were performed using Empyrean (Malvern Panalytical) (Cu-K $\alpha$  radiation, 45kV, 40mA, and 2 $\theta$  range of 10°–80°). A pH meter (Hanna edge pH) was used for the preparation of various pH solutions. The amount of dye adsorbed by hydrogels was determined using T80 + UV/VIS Spectrometer (PG Ins. Ltd.) with calibration graphs.

### Preparation and Characterization of Composite Hydrogel

p(AETAC)/AC composite hydrogels were prepared by the radical polymerization method, similar to our previous study, as given in the reaction scheme in Figure 1a (Onder et al., 2022). Briefly, 1 mL of AETAC and 1% mole of MBA (7.4 mg) based on the amount of monomer crosslinker were mixed in an ultrasonic bath. Various amounts of AC (50 mg, 75 mg, 100 mg, and 150 mg) were added to the medium and mixed in an ultrasonic bath until a homogeneous mixture was obtained. 50  $\mu$ L of TEMED was added to the reaction mixture. Finally, according to the mole amount of monomer, 1% APS was dissolved in 100  $\mu$ L deionized water and added to the reaction mixture, and polymerization was started. The resulting composite hydrogels were washed in distilled water for 24 h (3x8 h) to remove unreacted compounds. The swollen and washed p(AETAC)/AC composite hydrogels were cut. Then it was dried in a vacuum oven at 40 °C for 2 days. p(AETAC)/AC<sub>50</sub>, p(AETAC)/AC<sub>75</sub>, p(AETAC)/AC<sub>100</sub>, and p(AETAC)/AC<sub>150</sub> composite hydrogels obtained from 50, 75, 100, and 150 mg AC amounts were stored in a desiccator for adsorption experiments and characterization.

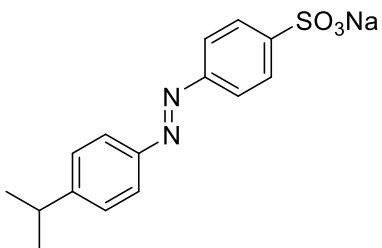
### Swelling and adsorption experiments

The gravimetric method was applied for the swelling characterization of composite hydrogels. For this purpose, the composite hydrogel containing different amounts of AC was kept in deionized water for 24 hours to determine the effect of the amount of AC on the swelling capacity of p(AETAC)/AC composite hydrogels. Final weights were measured to determine their swelling amount. Swelling capacities (ESR,  $g_{\text{water}}/g_{\text{hydrogel}}$ ) of p(AETAC)/AC composite hydrogels were calculated (Güngör & Ozay, 2022b). In addition, the effects of various waters (sea water (SW), river water (RW), synthetic textile waste (STWw), tap water (TW), and drinkable water (DbW)) on the swelling behavior of p(AETAC)/AC<sub>75</sub> composite hydrogel were investigated.

## Preparation of Cationic Composite Hydrogel Improved by Activated Carbon and Its Use in Removal of Anionic Dye

MO dye solution was used for anionic dye adsorption of p(AETAC)/AC<sub>75</sub> composite hydrogel from an aqueous medium. The chemical structure and properties of MO are shown in Table 1. The effects of initial dye concentration (in the range 25-1500 mg/L), contact time (0-24 h), dye solution pH (pH = 4, 5, 6, 7, 8, 9 and 10), temperature (30, 40, 50 ve 60 °C), and amount of adsorbent on the adsorption process were investigated for the removal of dyes from aqueous solutions. Here, 750 mg/L MO (pH=5.81 ± 0.2) aqueous solutions were used for the effect of adsorbent amount and temperature. At the same time, 500 mg/L MO aqueous solution was used to examine the effects of pH and contact time on adsorption. Equilibrium concentrations of MO ( $\lambda_{\max} = 464$  nm) dyestuff were measured with the help of a UV/Vis spectrophotometer. The adsorption capacity and dye removal percentages at equilibrium were calculated as in the literature (Onder et al., 2020).

**Table 1.** Characteristics of MO (Iwuozor et al., 2021)

Chemical structure of MO	Property	MO Dye
	IUPAC name	Sodium-4-(4-dimethylamino phenyl diazenyl) benzenesulfonate
	Molecular formula	C <sub>14</sub> H <sub>14</sub> N <sub>3</sub> SO <sub>3</sub> Na
	Molecular weight	327.34 g/mol
	pKa	3.4
	Colour & form	Orange-yellow powder & crystalline scales
	Melting point	> 300 °C
	Solubility	5 g/L (20 °C) in water

## RESULTS AND DISCUSSION

### Synthesis and Characterization of p(AETAC)/AC Composite Hydrogel

Removal of synthetic dyestuffs, which is one of the most important pollutants of usable water, is very important for a sustainable water economy. Therefore, p(AETAC)/AC composite hydrogels as a new adsorbent material were synthesized using the free-radical copolymerization method in four different AC amounts (Fig. 1a). The FT-IR spectrums of AC, AETAC monomer, and the prepared p(AETAC)/AC<sub>75</sub> composite hydrogel are given in Fig. 1b. In the spectrums of AC, AETAC, and composite hydrogel, absorption bands were determined at 3660-3100 cm<sup>-1</sup> and 3021 cm<sup>-1</sup>, respectively, because of -OH and C-H stretchings. In the FT-IR spectrum of the p(AETAC)/AC<sub>75</sub> composite hydrogel, the characteristic C=O stretch (1721 cm<sup>-1</sup>) of the AETAC monomer was observed (Wang et al., 2020; Ozsoy et al., 2022). In addition, N-H stretching (1640 cm<sup>-1</sup>) in the structure of crosslinker MBA and C-N stretching (955 cm<sup>-1</sup>) of quaternary ammonium groups in the structure of AETAC were observed (Wang et al., 2020; Ozsoy et al., 2022). The aromatic C=C stretch band in 1557 cm<sup>-1</sup> and the C-O stretch band at 1087 cm<sup>-1</sup> in the FT-IR spectrum of AC were determined in the FT-IR spectrum of the p(AETAC)/AC<sub>75</sub> composite hydrogel at 1577 cm<sup>-1</sup> and 1089 cm<sup>-1</sup> (Liu et al., 2017; Shu et al., 2017; Zhang et al., 2018). The FT-IR spectra show similar adsorption peaks with the p(AETAC)/AC<sub>75</sub> composite hydrogel, indicating that AETAC and AC have similar chemical properties. These results indicate that AC was successfully incorporated into the p(AETAC)/AC<sub>75</sub> composite hydrogel.

## Preparation of Cationic Composite Hydrogel Improved by Activated Carbon and Its Use in Removal of Anionic Dye

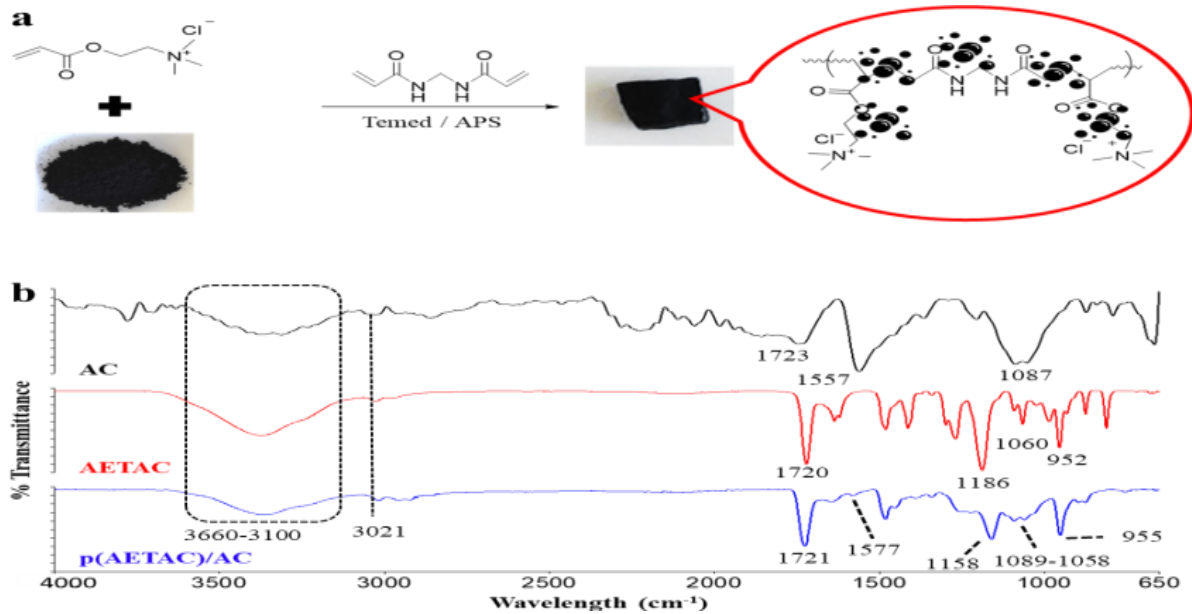


**Figure 1.** (a) Schematic Illustration of p(AETAC)/AC Composite Hydrogels Synthesis; (b) FT-IR Spectra of AC, AETAC and p(AETAC)/AC<sub>75</sub> Composite Hydrogel

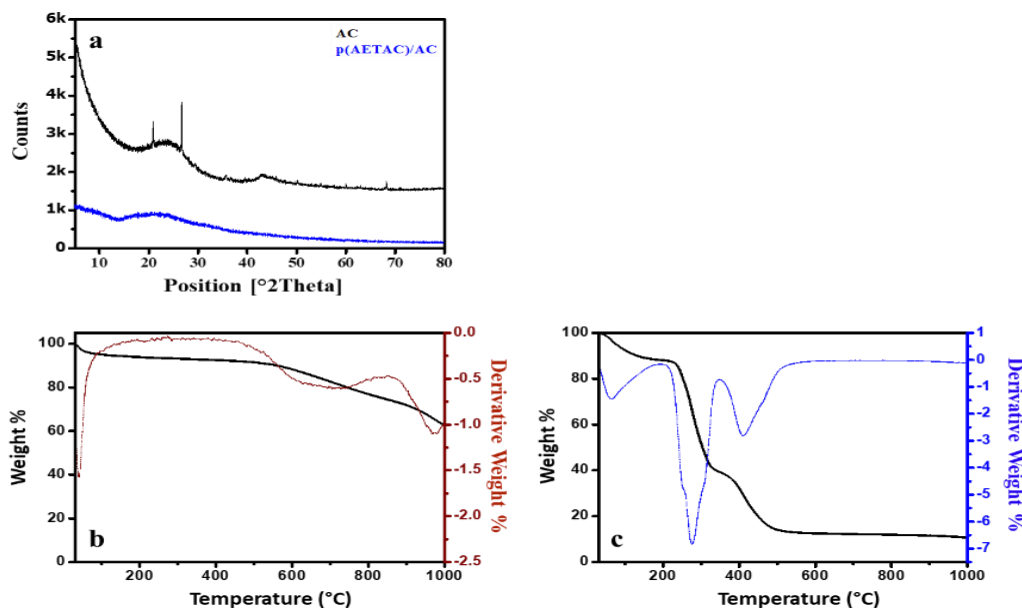


**Figure 2.** (a) XRD Spectra of AC and p(AETAC)/AC<sub>75</sub> Composite Hydrogel; TGA Thermograms of; (b) AC; (c) p(AETAC)/AC<sub>75</sub> Composite Hydrogel

The XRD patterns of the AC and p(AETAC)/AC<sub>75</sub> composite hydrogel are shown in Fig. 2a. The broad peaks at 23.65° and 43° of the commercial AC XRD model indicate the presence of an amorphous structure containing irregular carbon and planes, respectively. Moreover, sharp peaks of AC 20.90° ( $d=4.26$  Å), 26.70° ( $d=3.34$  Å), 36.55° ( $d=2.46$  Å), 39.50° ( $d=2.28$  Å), 50.18° ( $d=1.82$  Å), 59.99° ( $d=1.54$  Å), and 68.20° ( $d=1.37$  Å) show quartz 100, 101, 110, 102, 112, 211, and 203 respectively (Dutournié et al., 2019; Saafie et al., 2019; Bedia et al., 2020). These sharp peaks are related to the presence of quartz as an impurity (Dutournié et al., 2019). When the XRD pattern of p(AETAC)/AC<sub>75</sub> composite hydrogel was examined, it was determined that it had an amorphous structure. In addition, it was observed that the sharp peaks of AC disappeared within the amorphous structure of the p(AETAC)/AC<sub>75</sub> composite hydrogel. This may be a result of the homogeneous distribution of AC within the meshwork of the p(AETAC)/AC<sub>75</sub> composite hydrogel.

TGA thermograms of activated carbon and p(AETAC)/AC<sub>75</sub> composite hydrogel are shown in Fig. 2b and c. When the TGA and DTG thermograms of AC in Fig. 2b were examined, it was determined 3 decomposition stages with sharp at 40.58 °C and wide DTG endothermic peaks at 691.12 °C and 974.61 °C. These results showing that commercial activated carbon has good thermal stability are in agreement with the literature (Sharma et al., 2021). However, only 37.26% of the total mass was lost at 1000 °C. This may be due to impurities in the XRD spectrum of AC observed in Fig. 2a. The TGA thermogram of p(AETAC)/AC<sub>75</sub> composite hydrogel exhibited three specific gravity losses. Initial weight loss was observed below 200 °C and this could be attributed to water molecules. The rapid and significant mass decrease brought on by the breaking of polymer chains can be blamed for the second weight loss in the temperature range of 200–350 °C. The third weight loss in the 350-550 °C range can be attributed to a complex process dominated by the degradation of AETAC and thermally stable AC structures. Also, 89.33% of the total mass was lost after 1000 °C. The remaining 10.67% mass may be due to crystalline structures within it as determined in the XRD spectra of AC (Fig. 2a). All three degradation steps of the p(AETAC)/AC<sub>75</sub> composite hydrogel are consistent with the major peaks of the DTG curves. In the DTA curve of p(AETAC)/AC<sub>75</sub> composite hydrogel, an endothermic peak at 276.21 °C of depolymerization causing mass loss was observed. It can be said from the results that the incorporation of AC into the network structure results in the formation of a thermally stable composite hydrogel.

The morphological structure of the swollen p(AETAC)/AC<sub>75</sub> composite hydrogel, which was freeze-dried with the help of a lyophilizer, was examined by SEM. According to the SEM image in Fig. 3a, it was determined that the dry p(AETAC)/AC<sub>75</sub> composite hydrogel had pores ranging from approximately 10 µm to 100 µm. At the same time, AC in the p(AETAC)/AC<sub>75</sub> composite hydrogel were observed in the SEM image in Fig. 3b at ×20 000 magnification. SEM images show that the AC material is homogeneously dispersed in the p(AETAC)/AC composite hydrogel.

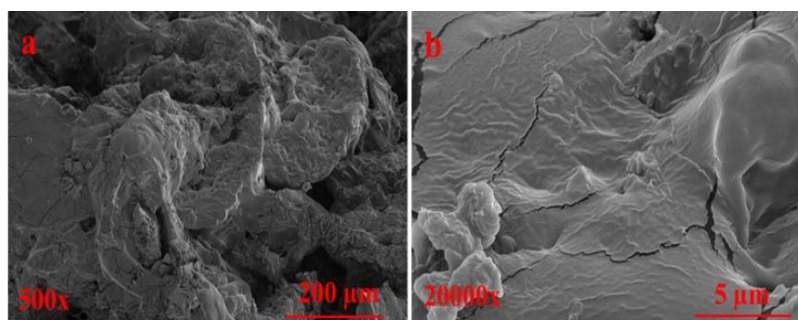


**Figure 3.** SEM Images of the p(AETAC)/AC<sub>75</sub> Composite Hydrogel at (a) 500x ; (b) 20 000x Magnifications

Swelling behavior is one of the most important factors affecting the efficiency of hydrogel systems used to remove impurities from water. Swelling, which is the most important feature of hydrogel systems, depends on the structure of the material. In deionized water, the effects of ambient pH and the quantity of AC on the swelling behavior of the p(AETAC)/AC<sub>75</sub> composite hydrogel were examined (~25 °C and 24 h). The effect of the amount of AC (50 mg, 75 mg, 100 mg, and 150 mg) on the swelling behavior of the composite hydrogels (p(AETAC)/AC<sub>50</sub>, p(AETAC)/AC<sub>75</sub>, p(AETAC)/AC<sub>100</sub>, and p(AETAC)/AC<sub>150</sub>) was determined and given in Fig. 4a. Equilibrium swelling values of p(AETAC)/AC<sub>50</sub>, p(AETAC)/AC<sub>75</sub>, p(AETAC)/AC<sub>100</sub>, and p(AETAC)/AC<sub>150</sub> composite hydrogels were  $41.29 \pm 0.32$  g<sub>water</sub>/g<sub>gel</sub>,  $80.26 \pm 5.58$  g<sub>water</sub>/g<sub>gel</sub>,  $187.18 \pm 17.04$  g<sub>water</sub>/g<sub>gel</sub> and  $278.47 \pm 73.27$  g<sub>water</sub>/g<sub>gel</sub>, respectively. Fig. 4a shows that as the amount of AC was raised, the composite hydrogel's swelling capability also rose. This is due to the fact that AC has a porous

structure. In addition, p(AETAC)/AC<sub>100</sub> and p(AETAC)/AC<sub>150</sub> composite hydrogels could not maintain their form due to excessive water retention at the equilibrium swelling point. The easy collection of adsorbent systems developed for water pollution is an important parameter in terms of its usefulness. Therefore, p(AETAC)/AC<sub>75</sub> composite hydrogel was chosen to be used in subsequent experiments.

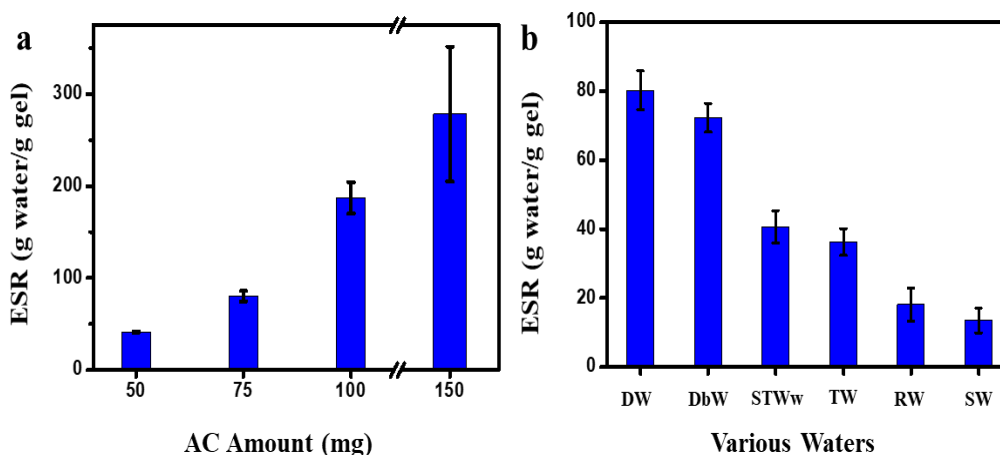


**Figure 4.** The effects of (a) AC Amount on Swelling Behavior of p(AETAC)/AC Composite Hydrogel and (b) pH on Swelling Behavior of p(AETAC)/AC Composite Hydrogel

Various waters containing different ion concentrations can affect the swelling ability of composite hydrogels (Güngör & Ozay, 2022b). On the swelling behavior of the p(AETAC)/AC<sub>75</sub> composite hydrogel, the effects of SW, RW, STWw, TW, and DbW were examined (**Fig. 4b**). Equilibrium swelling values of DW, DbW, STWw, TW, RW and SW were  $80.26 \pm 5.58$  g<sub>water</sub>/g<sub>gel</sub>,  $72.27 \pm 4.19$  g<sub>water</sub>/g<sub>gel</sub>,  $40.68 \pm 4.70$  g<sub>water</sub>/g<sub>gel</sub>,  $36.27 \pm 3.86$  g<sub>water</sub>/g<sub>gel</sub>,  $18.11 \pm 4.72$  g<sub>water</sub>/g<sub>gel</sub> and  $13.46 \pm 3.60$  g<sub>water</sub>/g<sub>gel</sub>, respectively. According to the equilibrium value of swelling in DW, a decrease in swelling values of DbW, STWw, TW, RW, and SW was determined. This situation was attributed to the decrease in swelling capacity with the effect of osmotic pressure in DbW, STWw, TW, RW, and SW environments containing different ion types. However, given that the p(AETAC)/AC<sub>75</sub> composite hydrogel with quaternary ammonium and porous AC has the capacity to swell in the STWw and is cross-linked, water-insoluble, and hydrophilic in nature, it could be a viable adsorbent for anionic dyes.

#### Adsorption studies of methyl orange by p(AETAC)/AC composite hydrogel

The adsorption behavior of p(AETAC)/AC<sub>75</sub> composite hydrogel, which was prepared and characterized as an adsorbent for anionic dyes in wastewater coming from the textile sector, was examined using anionic azo dyestuff MO. The effects of initial dye concentration, contact time, amount of adsorbent, pH, and temperature on the MO adsorption capacity of p(AETAC)/AC<sub>75</sub> composite hydrogel from aqueous solution were investigated.

The effect of MO initial dye concentration on the adsorption capacity of p(AETAC)/AC<sub>75</sub> composite hydrogel was determined at 8 different concentrations in the range of 25–1500 mg/L and is given in Fig. 5a. The p(AETAC)/AC<sub>75</sub> composite hydrogel has a high adsorption capacity up to 500 mg/L concentration, as shown in the Fig. 5a. However, the adsorption capacity of p(AETAC)/AC<sub>75</sub> composite hydrogel at 750 mg/L, 1000 mg/L, and 1500 mg/L concentrations was  $606.47 \pm 7.01$  mg/g,  $707.71 \pm 13.84$  mg/g ve  $836.24 \pm 15.42$  mg/g, respectively. The adsorption capacity of p(AETAC)/AC<sub>75</sub> composite hydrogel decreased with increasing initial MO concentration. This may be

due to the reduction in adsorption sites on the p(AETAC)/AC<sub>75</sub> composite hydrogel (Omorogie et al., 2022).

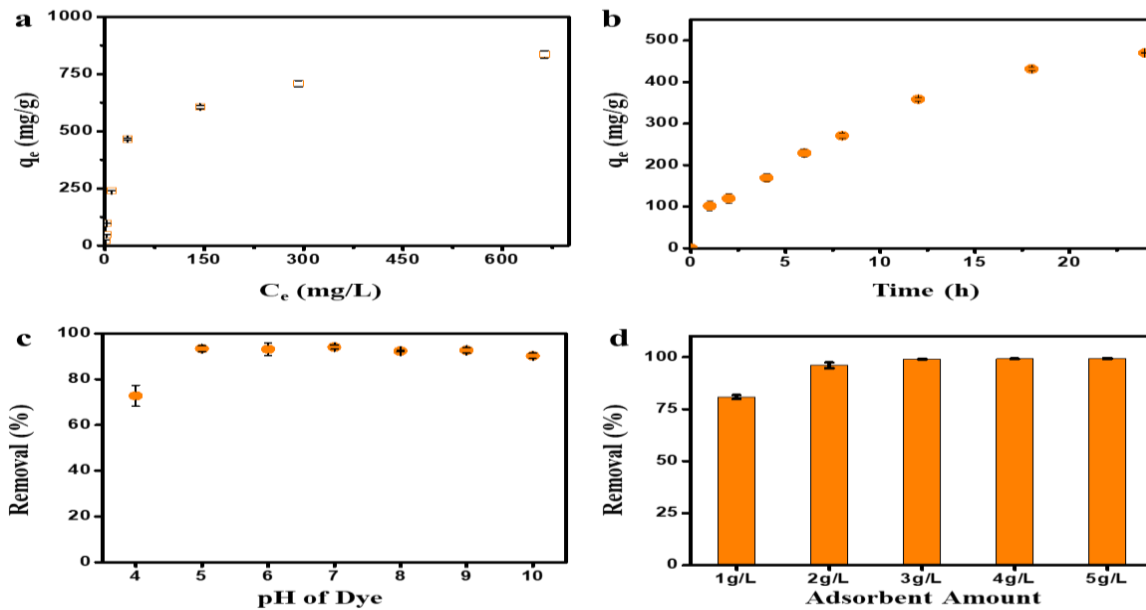


**Figure 5.** The Effect of (a) Initial Dye Concentration, (b) Contact Time, (c) pH of Dye, and (d) Adsorbent Amount on the MO Adsorption of p(AETAC)/AC<sub>75</sub> Composite Hydrogel

The effect of the contact time of the p(AETAC)/AC<sub>75</sub> composite hydrogel with the MO dye solution on the adsorption rate was investigated in 500 mg/L MO dye solution (pH=5.81 ± 0.2) at 30 °C over a time period of 1-24 h and presented in Fig. 5b (1 mg p(AETAC)/AC<sub>75</sub> / 1 mL MO). As the p(AETAC)/AC<sub>75</sub> composite hydrogel's contact time with the MO dye molecules lengthened, the likelihood of interaction between the dye molecules and the composite hydrogel rose. However, as the contact time increased, the adsorption equilibrium of the p(AETAC)/AC<sub>75</sub> composite hydrogel with the MO dye molecules began to occur and the adsorption rate slowed down.

Textile wastewater with various pH values can significantly affect the adsorption capacity of the adsorbent. For this reason, it is important to examine the adsorption behavior of the developed adsorbent materials in dye solutions at various pH values. The effect of the initial pH of MO aqueous solution on the adsorption behavior of p(AETAC)/AC<sub>75</sub> composite hydrogel was investigated in MO solution at pH=4, 5, 6, 7, 8, 9, and 10 at 24 h and 30 °C (Fig. 5c). The percentages of dye removal of p(AETAC)/AC<sub>75</sub> composite hydrogel from the MO dye solvents at pH= 4, 5, 6, 7, 8, 9, and 10 were 72.79%, 93.36%, 93.16%, 94.10%, 92.36%, 92.70% and 90.25%, respectively. At pH 5 to 10, the p(AETAC)/AC<sub>75</sub> composite hydrogel demonstrated a high dye removal rate. At pH 7, the p(AETAC)/AC<sub>75</sub> composite hydrogel had the highest percentage of MO removal. As the pH value increased, the percentage of dye removal decreased. The adsorption sites on the composite hydrogel might have affected the adsorption of anionic MO molecules because of the increased hydroxyl ion concentration (Onder et al. 2023). In addition, the percent of dye removal of the p(AETAC)/AC<sub>75</sub> composite hydrogel decreased at pH=4. The sodium sulfonate salt groups (-SOONa) in the MO dye molecules are changed into sulfonic acid (-SOOH) in acidic environments. Thus, by reducing the anion density at pH=4, the amount of dye removed from the p(AETAC)/AC<sub>75</sub> composite hydrogel may have decreased (Onder et al., 2020, 2023; Roa et al., 2021).

The effect of the amount of p(AETAC)/AC<sub>75</sub> composite hydrogel on the MO dye removal efficiency is given in Fig. 5d. Accordingly, 1-5 g of p(AETAC)/AC<sub>75</sub> composite hydrogel was kept in MO dye solution with a concentration of 750 mg/L (1 L) for 24 h and maximum dye removal amounts



were determined. As can be shown in Fig. 5d, as the amount of p(AETAC)/AC<sub>75</sub> composite hydrogel increased in accordance with the amount of MO used, nearly all of the MO was removed. This can be explained by the fact that when the amount of p(AETAC)/AC<sub>75</sub> composite hydrogel increases, there are more active regions interacting with MO dye molecules.

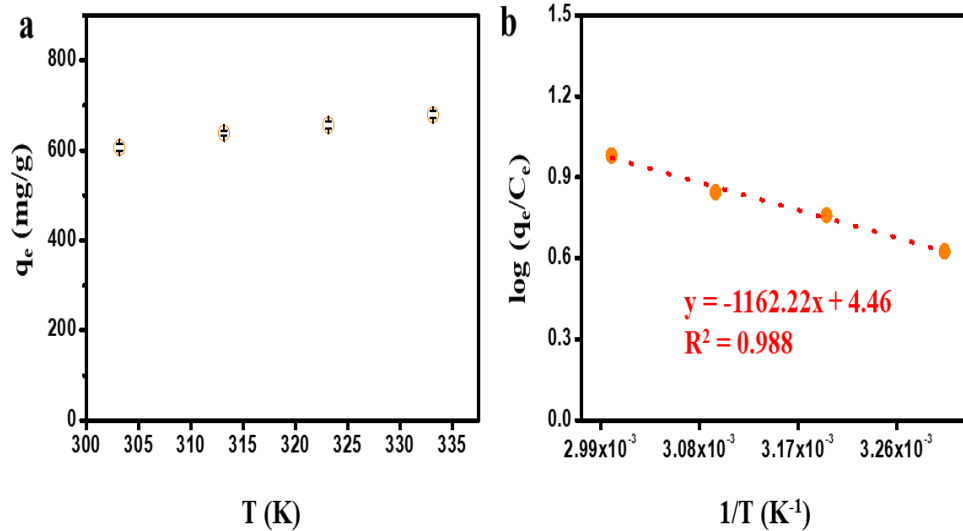


**Figure 6.** (a) Effect of Temperature on MO Adsorption of p(AETAC)/AC<sub>75</sub> Composite Hydrogel and (b) Plot of  $\ln(q_e/C_e)$  Versus  $1/T$  for Adsorption of MO

The effect of temperature on the adsorption of p(AETAC)/AC<sub>75</sub> composite hydrogel MO anionic azo dyestuff was performed at four different temperatures and 750 mg/L dye concentration. The data obtained are shown in Fig. 6a. In the presence of p(AETAC)/AC<sub>75</sub> composite hydrogel as adsorbent, when the temperature increased from 30 °C to 60 °C, the equilibrium adsorption amount of MO dyestuff increased from  $606.47 \pm 7.01$  to  $679.08 \pm 8.02$ , respectively. It demonstrates that when the temperature increases, the interaction between MO dye molecules and the p(AETAC)/AC<sub>75</sub> composite hydrogel raises. The thermodynamic parameters (Enthalpy- $\Delta H^\circ$ ; entropy- $\Delta S^\circ$ ; Gibbs free energy- $\Delta G^\circ$ ) for the adsorption of the MO dyestuff of the p(AETAC)/AC<sub>75</sub> composite hydrogel were calculated using Eq. (1) and (2) below, and the graph of Fig. 6b was obtained (Güngör & Ozay, 2022b; Ozsoy et al., 2022). All values are given in Table 2.

$$\log\left(\frac{q_e}{C_e}\right) = \frac{\Delta S^\circ}{2.303R} - \frac{\Delta H^\circ}{2.303RT} \quad (1)$$

$$\Delta G^\circ = \Delta H^\circ - T\Delta S^\circ \quad (2)$$

When the thermodynamic parameters in Table 2 are examined, the  $\Delta G^\circ$  value less than zero at four different temperatures indicates that the dye adsorption is spontaneous.  $0 < \Delta H^\circ$  indicates the endothermic nature of the adsorption process, while  $0 < \Delta S^\circ$  indicates increased disorder at the composite hydrogel and solution interface.

**Table 2.** Thermodynamic Parameters for p(AETAC)/AC<sub>75</sub> Composite Hydrogel

Thermodynamic Parameters	Unit	MO Dye	
$\Delta H^\circ$	kJ/mol	$22.25 \pm 1.43$	
$\Delta S^\circ$	J/mol.K	$85.40 \pm 4.60$	
$\Delta G^\circ$	303.15 K	kJ/mol	-3.63
	313.15 K	kJ/mol	-4.49
	323.15 K	kJ/mol	-5.34
	333.15 K	kJ/mol	-6.20

### Adsorption isotherms and kinetics

It is important to find the most suitable adsorption isotherm model to determine the interactions between dye molecules and adsorbent and thus to design adsorption systems (Ayawei et al., 2017). In this study, Langmuir and Freundlich isotherm models were applied with the help of linear equations in the literature (Bulut et al., 2008a; Ozsoy et al., 2022). The graphs obtained for the Langmuir and Freundlich isotherms are presented in Fig. 7a and b. The parameters of the isotherm models corresponding to the MO dye adsorption of p(AETAC)/AC<sub>75</sub> composite hydrogel were calculated from the graphs shown in Fig. 7a and b and given in Table 3.

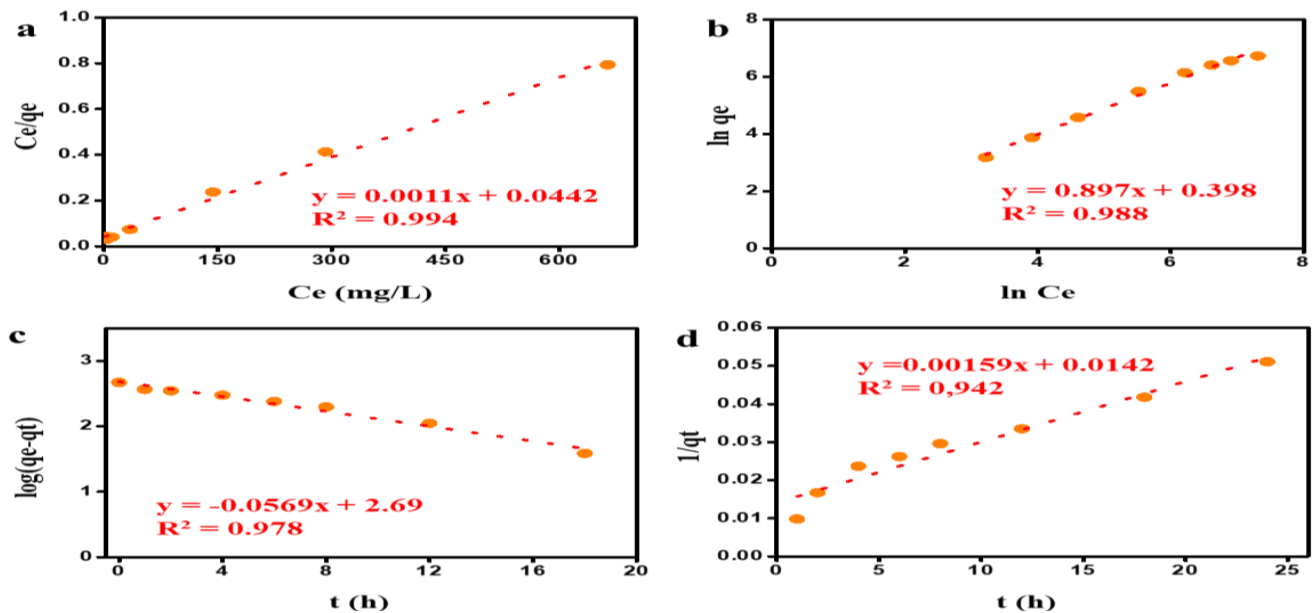


**Figure 7.** (a) Langmuir, (b) Freundlich Isotherm Models Plots and (c) Pseudo First-Order Model, and (a) Pseudo Second-Order Model for Adsorption of MO Dye by the p(AETAC)/AC<sub>75</sub> Composite Hydrogel

**Table 3.** Isotherm and Kinetic Parameters for p(AETAC)/AC<sub>75</sub> Composite Hydrogel

Isotherms and Kinetics Models	Unit	Isotherm Models		Kinetic Models	
		Langmuir	Freundlich	PFO	PSO
$q_m$	mg/g	909.09			
$K_L$	L/mg	0.0249			
$R_L$		0.62-0.03			
$K_f$	mg/g		1.49		
$n$			1.11		
$q_e$	mg/g			489.78	628.93
$k_1$	1/h			0.13	
$k_2$	g/mg.h				1.78E-4
$R^2$		0.994	0.988	0.984	0.942

According to Table 3, it was determined that the p(AETAC)/AC<sub>75</sub> composite hydrogel MO complied with the Langmuir isotherm model according to the regression ( $R^2$ ) values for the dye adsorption processes. According to the Langmuir isotherm model, which expresses monolayer adsorption, the maximum adsorption capacity for MO of the p(AETAC)/AC<sub>75</sub> composite hydrogel is 909.09 mg/g (Table 3). The separation factor values ( $R_L$ ) of the Langmuir isotherm in Table 3 range from 0 to 1 ( $R_L > 1$ , Unfavourable;  $R_L = 1$ , linear;  $0 < R_L < 1$ , favourable;  $R_L = 0$ , irreversible). This indicates the strong affinity between the p(AETAC)/AC<sub>75</sub> composite hydrogel and the MO anionic azo

dye. It also shows moderately difficult adsorption of the p(AETAC)/AC<sub>75</sub> composite hydrogel for MO relative to n obtained by the Freundlich isotherm model (Table 3).

Determining the potential rate control steps of the adsorption dynamics between the p(AETAC)/AC<sub>75</sub> composite hydrogel and the MO anionic azo dye by kinetic studies is important for designing adsorption systems. The adsorption kinetic model was established using pseudo-first order (PFO) and pseudo-second order (PSO) kinetic models (Fig. 7c and d). Kinetic parameters (Table 3) were obtained with graphs (Figure 7c ve d) created with the help of equations in the literature (Bulut et al., 2008b; Ilgin et al., 2023). Considering the R<sup>2</sup> values given in Table 3 for the adsorption of MO anionic azo dyestuff with p(AETAC)/AC<sub>75</sub> composite hydrogel, it was determined that the PFO kinetic model fit better than the PSO kinetic model. In addition, the calculated q<sub>e</sub> value for PFO was closer to the experimental value. The PFO model assumes that physical adsorption limits the rate of adsorption, while the PSO model assumes that chemical adsorption limits the rate of adsorption. Thus the p(AETAC)/AC<sub>75</sub> composite hydrogel is decisive in the rate control step of physisorption, in the adsorption of MO anionic azo dyestuff.

**Table 4.** Comparison of MO Adsorption Capacities of Different Adsorbents in the Literature

Adsorbents	Unit	Maximum adsorption capacity	References
Halloysite nanotubes		13.56	(Wu et al., 2021)
Chrysotile nanotubes		31.46	
The anionic Amberlite®IRA-410 resin		188.2	(Elabboudi et al., 2023)
Polymeric ionic liquid-graphene oxide-TiO <sub>2</sub> /Fe <sub>3</sub> O <sub>4</sub>	mg/g	67.88	(Liu et al., 2023)
Anchote peel		103.03	(Hambisa et al., 2022)
p(AETAC)/AC <sub>75</sub>		909.09	<b>In study</b>

The maximum adsorption capacities of different adsorbents used to remove MO dye from aqueous solutions in the literature are given in Table 4. As shown in Table 4, the developed composite hydrogel has a relatively high adsorption capacity compared to many adsorbents in the literature. At the same time, the fact that the composite hydrogel has an efficient, cheap, and easy production process shows the potential to be a competitive adsorbent.

## CONCLUSION

The water-insoluble and quaternary ammonium-containing p(AETAC)/AC<sub>75</sub> composite hydrogel was obtained by free radical polymerization with MBA crosslinker from AETAC and AC. It was characterized by FT-IR, TGA, XRD, and SEM methods. p(AETAC)/AC<sub>75</sub> composite hydrogel demonstrated swelling ability in STWw. The p(AETAC)/AC<sub>75</sub> composite hydrogel had high MO adsorption ability over a wide pH. The adsorption data agree with the Langmuir isotherm model and the PFO kinetic model. The maximum adsorption ability of p(AETAC)/AC<sub>75</sub> composite hydrogel according to Langmuir isotherm was 909.09 mg/g. According to the obtained thermodynamic parameters, the adsorption is spontaneous and endothermic. The p(AETAC)/AC<sub>75</sub> composite hydrogel showed excellent performance for the removal of MO, the anionic azo dyestuff. p(AETAC)/AC<sub>75</sub> composite hydrogel may have significant potential for removing anionic dyes that pollute water.

## ACKNOWLEDGEMENTS

I would like to thank Prof. Dr. Hava ÖZAY and Prof. Dr. Özgür ÖZAY for their support.

## REFERENCES

- Abutaleb, A., Imran, M., Zouli, N., Khan, A. H., Hussain, S., Ali, M. A., Zahmatkesh, S. (2023). Fe<sub>3</sub>O<sub>4</sub>-multiwalled carbon nanotubes-bentonite as adsorbent for removal of methylene blue from aqueous solutions. *Chemosphere*, 316(January), 137824. <https://doi.org/10.1016/j.chemosphere.2023.137824>
- Anirudhan, T. S., Mohan, M., & Rajeev, M. R. (2022). Modified chitosan-hyaluronic acid based hydrogel for the pH-responsive Co-delivery of cisplatin and doxorubicin. *Int. J. Biol. Macromol.*, 201, 378–388. <https://doi.org/10.1016/j.ijbiomac.2022.01.022>
- Ayawei, N., Ebelegi, A. N., & Wankasi, D. (2017). Modelling and Interpretation of Adsorption Isotherms. *Journal of Chemistry*, 2017. <https://doi.org/10.1155/2017/3039817>
- Bedia, J., Peñas-Garzón, M., Gómez-Avilés, A., Rodríguez, J. J., & Bolver, C. (2020). Review on Activated Carbons by Chemical Activation with FeCl<sub>3</sub>. *C — Journal of Carbon Research*, 6(2), 21. <https://doi.org/10.3390/c6020021>
- Bulut, E., Özacar, M., Şengil, İ.A. (2008a). Adsorption of malachite green onto bentonite: Equilibrium and kinetic studies and process design. *Microporous Mesoporous Mater.*, 115, 3, 234-246. <https://doi.org/10.1016/j.micromeso.2008.01.039>
- Bulut, E., Özacar, M., Şengil, İ.A. (2008b). Equilibrium and kinetic data and process design for adsorption of Congo Red onto bentonite. *J. Hazard. Mater.*, 154, 1–3, 613-622. <https://doi.org/10.1016/j.jhazmat.2007.10.071>
- Chowdhury, A., Kumari, S., Khan, A. A., & Hussain, S. (2020). Selective removal of anionic dyes with exceptionally high adsorption capacity and removal of dichromate (Cr<sub>2</sub>O<sub>7</sub><sup>2-</sup>) anion using Ni-Co-S/CTAB nanocomposites and its adsorption mechanism. *J. Hazard. Mater.*, 385(September 2019), 121602. <https://doi.org/10.1016/j.jhazmat.2019.121602>
- Dutournié, P., Bruneau, M., Brendlé, J., Limousy, L., Pluchon, S. (2019). Mass transfer modelling in clay-based material: Estimation of apparent diffusivity of a molecule of interest. *Comptes Rendus Chimie*, 22, 2–3, 250-257. <https://doi.org/10.1016/j.crci.2018.10.008>
- Elabboudi, M., Bensalah, J., El-Amri, A., El-Azzouzi, N., Srhir, B., Lebkiti, A., Zarrouk, A., Rifi, E.H. (2023). Adsorption performance and mechanism of anionic MO dye by the adsorbent polymeric Amberlite®IRA-410 resin from environment wastewater: Equilibrium kinetic and thermodynamic studies. *J. Mol. Struct.*, 1277, 134789. <https://doi.org/10.1016/j.molstruc.2022.134789>
- Glaas-WHO. (2022). Strong systems and sound investments: evidence on and key insights into accelerating progress on sanitation, drinking-water and hygiene. The UN-Water global analysis and assessment of sanitation and drinking-water (GLAAS) 2022 report, Licence CC BY-NC-SA 3.0 IGO.
- Güngör, Z., & Ozay, H. (2022a). Ultra-fast pH determination with a new colorimetric pH-sensing hydrogel for biomedical and environmental applications. *Reactive and Functional Polymers*, 180(September). <https://doi.org/10.1016/j.reactfunctpolym.2022.105398>
- Güngör, Z., & Ozay, H. (2022b). Use of cationic p[2-(acryloyloxy)ethyl] trimethylammonium chloride in hydrogel synthesis and adsorption of methyl orange with jeffamine based crosslinker. *J. Dispers Sci. Technol.*, 0(0), 1–16. <https://doi.org/10.1080/01932691.2022.2129676>
- Hambisa, A.A., Regasa, M.B., Ejigu, H.G., Senbeto C.B. (2023). Adsorption studies of methyl orange dye removal from aqueous solution using Anchote peel-based agricultural waste adsorbent. *Appl Water Sci* 13, 24. <https://doi.org/10.1007/s13201-022-01832-y>

- Ilgin, P., Onder, A., Kıvanç, M. R., Ozay, H., & Ozay, O. (2023). Adsorption of methylene blue from aqueous solution using poly(2-acrylamido-2-methyl-1-propanesulfonic acid-co-2-hydroxyethyl methacrylate) hydrogel crosslinked by activated carbon. *J. Macromol. Sci. A*, 60, 135–144. <https://doi.org/10.1080/10601325.2023.2165945>
- Iwuozor, K.O, Ighalo, J.O., Emenike, E.C., Ogunfowora, L.A., Igwegbe, C.A. (2021). Adsorption of methyl orange: A review on adsorbent performance. *Curr. Opin. Green Sustain. Chem.*, 4, 100179. <https://doi.org/10.1016/j.crgsc.2021.100179>
- Jiang, Y., Liu, B., Xu, J., Pan, K., Hou, H., Hu, J., & Yang, J. (2018). Cross-linked chitosan/ $\beta$ -cyclodextrin composite for selective removal of methyl orange: Adsorption performance and mechanism. *Carbohydrate Polymers*, 182(July 2017), 106–114. <https://doi.org/10.1016/j.carbpol.2017.10.097>
- Kim, S. H., Kim, D. S., Moradi, H., Chang, Y. Y., & Yang, J. K. (2023). Highly porous biobased graphene-like carbon adsorbent for dye removal: Preparation, adsorption mechanisms and optimization. *J. Environ. Chem. Eng.*, 11(2), 109278. <https://doi.org/10.1016/j.jece.2023.109278>
- Liu, H., Wang, K., Zhang, D., Zhao, D., Zhai, J., Cui, W. (2023). Adsorption and catalytic removal of methyl orange from water by PIL-GO/TiO<sub>2</sub>/Fe<sub>3</sub>O<sub>4</sub> composites. *Mater Sci Semicond Process.* 154, 107215. <https://doi.org/10.1016/j.mssp.2022.107215>
- Liu, Y., Liu, X., Dong, W., Zhang, L., Kong, Q., & Wang, W. (2017). Efficient Adsorption of Sulfamethazine onto Modified Activated Carbon: A Plausible Adsorption Mechanism. *Scientific Reports*, 7(1), 1–12. <https://doi.org/10.1038/s41598-017-12805-6>
- Omorie, M. O., Agbadaola, M. T., Olatunde, A. M., Helmreich, B., & Babalola, J. O. (2022). Surface equilibrium and dynamics for the adsorption of anionic dyes onto MnO<sub>2</sub>/biomass micro-composite. *Green Chemistry Letters and Reviews*, 15(1), 49–58. <https://doi.org/10.1080/17518253.2021.2018508>
- Onder, A. & Ozay, H. (2021). Highly efficient removal of methyl orange from aqueous media by amine functional cyclotriphosphazene submicrospheres as reusable column packing material. *Chem. Eng. Process.: Process Intensif.*, 165, 108427. <https://doi.org/10.1016/J.CEP.2021.108427>
- Onder, A., Ilgin, P., Ozay, H., & Ozay, O. (2020). Removal of dye from aqueous medium with pH-sensitive poly[(2-(acryloyloxy)ethyl)trimethylammonium chloride-co-1-vinyl-2-pyrrolidone] cationic hydrogel. *J. Environ. Chem. Eng.*, 8(5), 104436. <https://doi.org/10.1016/j.jece.2020.104436>
- Onder, A., Ilgin, P., Ozay, H., & Ozay, O. (2022). Preparation of composite hydrogels containing fly ash as low-cost adsorbent material and its use in dye adsorption. *Int. J. Environ. Sci. Technol.*, 19, 7031–7048. <https://doi.org/10.1007/s13762-021-03622-6>
- Onder, A., Kıvanç, M. R., Ilgin, P., Ozay, H., & Ozay, O. (2023). Synthesis of p(HEMA-co-AETAC) nanocomposite hydrogel with vinyl-function montmorillonite nanoparticles and effective removal of methyl orange from aqueous solution. *J. Macromol. Sci. A*, 60(2), 108–123. <https://doi.org/10.1080/10601325.2023.2169155>
- Ozsoy, F., Ozdilek, B., Onder, A., Ilgin, P., Ozay, H., & Ozay, O. (2022). Graphene nanoplate incorporated Gelatin/poly(2-(Acryloyloxy)ethyl trimethylammonium chloride) composites hydrogel for highly effective removal of Alizarin Red S from aqueous solution. *Journal of Polymer Research*, 29(11). <https://doi.org/10.1007/s10965-022-03327-5>

- Roa, K., Tapiero, Y., Thotiyl, M. O., & Sánchez, J. (2021). Hydrogels based on poly([2-(acryloxy)ethyl] trimethylammonium chloride) and nanocellulose applied to remove methyl orange dye from water. *Polymers*, 13(14). <https://doi.org/10.3390/polym13142265>
- Rong, N., Chen, C., Ouyang, K., Zhang, K., Wang, X., & Xu, Z. (2021). Adsorption characteristics of directional cellulose nanofiber/chitosan/montmorillonite aerogel as adsorbent for wastewater treatment. *Sep. Purif. Technol.*, 274, 119120. <https://doi.org/10.1016/j.seppur.2021.119120>
- Saafie, N., Samsudin, M. F. R., Sufian, S., & Ramli, R. M. (2019). Enhancement of the activated carbon over methylene blue removal efficiency via alkali-acid treatment. *AIP Conference Proceedings*, 2124(July). <https://doi.org/10.1063/1.5117106>
- Sharma, S., Kaur, M., Sharma, C., Choudhary, A. and Paul, S. (2021). Biomass-Derived Activated Carbon-Supported Copper Catalyst: An Efficient Heterogeneous Magnetic Catalyst for Base-Free Chan–Lam Coupling and Oxidations. *ACS Omega*, 6, 30, 19529–19545. <https://doi.org/10.1021/acsomega.1c01830>
- Shu, J., Cheng, S., Xia, H., Zhang, L., Peng, J., Li, C., & Zhang, S. (2017). Copper loaded on activated carbon as an efficient adsorbent for removal of methylene blue. *RSC Advances*, 7(24), 14395–14405. <https://doi.org/10.1039/c7ra00287d>
- Singh, A., Kar, A. K., Singh, D., Verma, R., Shraogi, N., Zehra, A. et al. (2022). pH-responsive eco-friendly chitosan modified cenosphere/alginate composite hydrogel beads as carrier for controlled release of Imidacloprid towards sustainable pest control. *J. Chem. Eng*, 427, 131215. <https://doi.org/10.1016/j.cej.2021.131215>
- Sugawara, A., Asoh, T. A., Takashima, Y., Harada, A., & Uyama, H. (2020). Composite hydrogels reinforced by cellulose-based supramolecular filler. *Polym. Degrad. Stab.*, 177, 109157. <https://doi.org/10.1016/j.polymdegradstab.2020.109157>
- Tian, H., Guo, Q., & Xu, D. (2010). Hydrogen generation from catalytic hydrolysis of alkaline sodium borohydride solution using attapulgite clay-supported Co-B catalyst. *Journal of Power Sources*, 195(8), 2136–2142. <https://doi.org/10.1016/J.JPOWSOUR.2009.10.006>
- Wang, L., Zhang, X., Xu, J., Wang, Q., & Fan, X. (2020). Synthesis of partly debranched starch-g-poly(2-acryloyloxyethyl trimethyl ammonium chloride) catalyzed by horseradish peroxidase and the effect on adhesion to polyester/cotton yarn. *Process Biochemistry*, 97(March), 176–182. <https://doi.org/10.1016/j.procbio.2020.07.015>
- Wu, L., Liu, X., Lv, G. et al. (2021). Study on the adsorption properties of methyl orange by natural one-dimensional nano-mineral materials with different structures. *Sci Rep* 11, 10640. <https://doi.org/10.1038/s41598-021-90235-1>
- Xu, H., Zhang, Y., Cheng, Y., Tian, W., Zhao, Z., & Tang, J. (2019). Polyaniline/attapulgite-supported nanoscale zero-valent iron for the rival removal of azo dyes in aqueous solution. *Adsorp Sci Technol*, 37(3–4), 217–235. <https://doi.org/10.1177/0263617418822917>
- Zhang, L., Tu, L. Y., Liang, Y., Chen, Q., Li, Z. S., Li, C. H., Li, W. (2018). Coconut-based activated carbon fibers for efficient adsorption of various organic dyes. *RSC Advances*, 8(74), 42280–42291. <https://doi.org/10.1039/c8ra08990f>